

Chiral phase transition in (2 + 1)-flavor QCD

Heng-Tong Ding¹, Prasad Hegde², Olaf Kaczmarek^{1,3}, Frithjof Karsch^{3,4}, Anirban Lahiri³, Sheng-Tai Li^{*1†}, Swagato Mukherjee⁴, Peter Petreczky⁴ (for the HotQCD collaboration)

¹ Key Laboratory of Quark & Lepton Physics (MOE) and Institute of Particle Physics, Central China Normal University, Wuhan 430079, China.

² Center for High Energy Physics, Indian Institute of Science, Bangalore 560012, India

³ Fakultät für Physik, Universität Bielefeld, D-33615 Bielefeld, Germany

⁴ Physics Department, Brookhaven National Laboratory, Upton, NY 11973, USA

E-mail: hengtong.ding@mail.ccnu.edu.cn, prasadhegde@iisc.ac.in, okacz@physik.uni-bielefeld.de, karsch@physik.uni-bielefeld.de, alahiri@physik.uni-bielefeld.de, lishengtai@mails.ccnu.edu.cn, swagato@bnl.gov, petreczk@quark.phy.bnl.gov

The chiral phase transition temperature T_c^0 is a fundamental quantity of QCD. To determine this quantity we have performed simulations of (2 + 1)-flavor QCD using the Highly Improved Staggered Quarks (HISQ/tree) action on $N_\tau = 6, 8$ and 12 lattices with aspect ratios N_σ/N_τ ranging from 4 to 8. In our simulations the strange quark mass is fixed to its physical value m_s^{phy} , and the values of two degenerate light quark masses m_l are varied from $m_s^{\text{phy}}/20$ to $m_s^{\text{phy}}/160$ which correspond to a Goldstone pion mass m_π ranging from 160 MeV to 55 MeV in the continuum limit. By investigating the light quark mass dependence and the volume dependence of various chiral observables, e.g. chiral susceptibilities and Binder cumulants, no evidence for a first order phase transition in our current quark mass window is found. Two estimators T_{60} and T_δ are proposed to extract the chiral phase transition temperature T_c^0 in the chiral and continuum limit and our current estimate for T_c^0 is 132_{-6}^{+3} MeV.

The 36th Annual International Symposium on Lattice Field Theory - LATTICE2018
22-28 July, 2018

Michigan State University, East Lansing, Michigan, USA.

*Speaker.

†This work was supported in part by the Deutsche Forschungsgemeinschaft (DFG) through the grant 315477589-TRR 211, the grants 05P15PBCAA and 05P18PBCA1 of the German Bundesministerium für Bildung und Forschung, the National Natural Science Foundation of China under grant numbers 11775096 and 11535012, Furthermore, this work was supported through Contract No. DE-SC0012704 with the U.S. Department of Energy, through the Scientific Discovery through Advanced Computing (SciDAC) program funded by the U.S. Department of Energy, Office of Science, Advanced Scientific Computing Research and Nuclear Physics and the DOE Office of Nuclear Physics funded BEST topical collaboration, and a Early Career Research Award of the Science and Engineering Research Board of the Government of India. Numerical calculations have been made possible through PRACE grants at CSCS, Switzerland, and at CINECA, Italy as well as grants at the Gauss Centre for Supercomputing and NIC-Jülich, Germany. These grants provided access to resources on Piz Daint at CSCS, Marconi at CINECA as well as on JUQUEEN and JUWELS at NIC. Additional calculations have been performed on GPU clusters of USQCD, at Bielefeld University, the PC² Paderborn University and the Nuclear Science Computing Center at Central China Normal University, Wuhan, China. Some data sets have also partly been produced at the TianHe II Supercomputing Center in Guangzhou.

1. Introduction

One of the basic goals of lattice QCD calculations at non-zero temperature is to understand the QCD phase diagram [1]. At zero baryon chemical potential, the QCD phase structure may depend on the number of light quark flavors [2] which is summarized in the Columbia plot in two scenarios as shown in Fig. 1. It is concluded that the physical point $(m_{u,d}^{\text{phy}}, m_s^{\text{phy}})$ is located in the crossover region [3, 4, 5]. The first order phase transition regions and the crossover region are separated by second order phase transition lines which belong to the $Z(2)$ universality class. In the chiral limit of $N_f = 2$ theory, if $U_A(1)$ symmetry remains broken at the chiral transition temperature, the chiral phase transition is a second order phase transition belonging to an $O(4)$ universality class [2]. Thus the chiral first order region in the left bottom corner of Columbia plot, the second order $O(4)$ line for $N_f = 2$ case and the second order $Z(2)$ line are supposed to meet at a tri-critical point m_s^{tri} . The location of the tri-critical point is still an open question. It is possible that the tri-critical point shifts to infinite strange quark mass [6]. The nature of the chiral phase transition at zero baryon

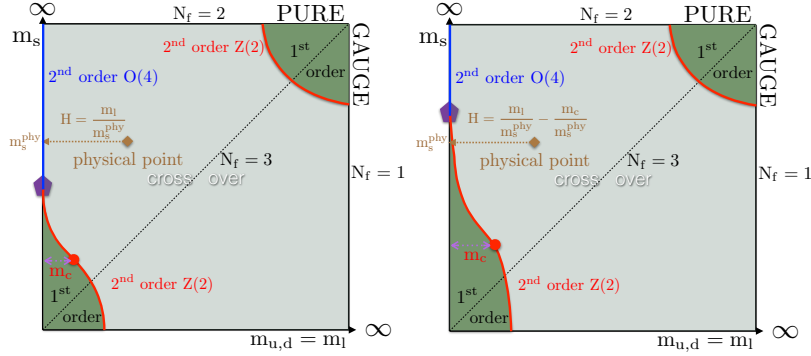


Figure 1: Schematic QCD phase structure with different values of quark masses $(m_{u,d}, m_s)$ at zero baryon number density for $m_s^{\text{tri}} < m_s^{\text{phy}}$ (left) and $m_s^{\text{tri}} > m_s^{\text{phy}}$ (right).

chemical potential is also relevant for our understanding of the QCD phase diagram at non-zero chemical potential. If $m_s^{\text{tri}} < m_s^{\text{phy}}$, it is expected that in the chiral limit there will be a second order phase transition which belongs to the $O(4)$ universality class as seen from the Fig. 1 (left). In this case, in the chiral limit, there might exist a tri-critical point as if QCD system becomes a first order phase transition in large baryon chemical potential. If $m_s^{\text{tri}} > m_s^{\text{phy}}$, towards the chiral limit the system passes through the $Z(2)$ critical line to a first order phase transition region as shown in Fig. 1 (right). In this case the chiral phase transition may be first order for all values of the chemical potential or, there may exist a critical point such that the transition becomes a crossover transition at large baryon chemical potential.

In this proceedings, we focus on the determination of the chiral phase transition temperature T_c^0 in the chiral limit and continuum limit, and we will also discuss the nature of the chiral phase transition. Previous studies have been reported in Ref. [7, 8, 9].

2. Observables and definitions

The universal behavior of the order parameter M and its susceptibility χ_M can be described by

the so-called Magnetic Equation of State (MEOS) [10] as follows

$$M(t, h) = h^{1/\delta} f_G(z) \quad \text{and} \quad \chi_M(t, h) = \frac{\partial M}{\partial H} = h_0^{-1} h^{1/\delta-1} f_\chi(z). \quad (2.1)$$

Here $z = th^{-1/\beta\delta}$ is a scaling variable, $t = \frac{1}{t_0} \frac{T-T_c^0}{T_c^0}$ is the reduced temperature and $h = H/h_0 = \frac{m_l}{m_s}/h_0$ is the symmetry breaking field. β , δ are universal critical exponents which are unique for a given universality class as shown in Table 1.

Model	β	δ	z_p	z_{60}	$f_G(z_p)$	$f_\chi(z_p)$
Z(2)	0.3258	4.805	2.00(5)	0.10(1)	0.548(10)	0.3629(1)
O(2)	0.349	4.780	1.58(4)	-0.005(9)	0.550(10)	0.3489(1)
O(4)	0.380	4.824	1.37(3)	-0.013(7)	0.532(10)	0.3430(1)

Table 1: Universal critical exponents β , δ for Z(2), O(2) and O(4) 3-d universality classes. Also given is the peak location of f_χ , i.e. z_p , and the location z_{60} where the height of the f_χ is 60% of its peak height and the values of $f_G(z_p)$ and $f_\chi(z_p)$.

Three non-universal parameters h_0 , t_0 , T_c^0 are unique for a particular system, e.g. T_c^0 is the critical temperature of chiral phase transition in the light quark chiral limit. For scaling variable z_X , it is related to a temperature T_X as follows

$$T_X(H) = T_c^0 + z_X T_c^0 H^{1/\beta\delta} / z_0, \quad z_0 = h_0^{1/\beta\delta} / t_0. \quad (2.2)$$

At the peak location of f_χ , i.e. $z_X = z_p$, we have the relationship between pseudo-critical temperature T_{pc} and the critical temperature T_c^0 , e.g. $T_{pc} = T_c^0 + z_p T_c^0 H^{1/\beta\delta} / z_0$. Here we analyze two other estimators for the chiral phase transition temperature, defined by two specific values of the scaling variable z , i.e. z_{60} and z_δ . The former is defined by $f_\chi(z_{60}) = 0.6 f_\chi(z_p)$ with $z_{60} < z_p$ and the corresponding T_{60} is defined as $\chi_M(T_{60}) = 0.6 \chi_M(T_{pc})$ with $T_{60} < T_{pc}$.

Since z_{60} is very close to zero the H -dependent term in Eq. 2.2 is suppressed by at least by an order of magnitude compared to z_p . This is shown in the left panel of Fig. 2 and Table 1, for relevant universality classes. We thus can estimate T_c^0 by investigating the values of T_{60} as follows

$$T_{60}(H) = T_c^0 + z_{60} T_c^0 H^{1/\beta\delta} / z_0, \quad (2.3)$$

In the right panel of Fig.2, we plot f_χ/f_G vs. $(T - T_c^0)/T_c^0$ for O(4) universality class where we have set $z_0=1$ for simplicity. The different curves, corresponding to different H , meet at a unique crossing point $(0, 1/\delta)$ [11]. This thus drives us to estimate T_c^0 by looking at $H\chi_M/M$,

$$\frac{H\chi_M(T_\delta, V, H)}{M(T_\delta, V, H)} = \frac{1}{\delta} \Rightarrow T_c^0 = \lim_{H \rightarrow 0} \lim_{V \rightarrow \infty} T_\delta(V, H). \quad (2.4)$$

As shown in Eq. 2.4, T_c^0 can be estimated by looking at $T_\delta(V, H)$ in the infinite volume limit and chiral limit.

By looking at following equation we will be able to investigate the nature of chiral phase transition

$$\frac{M}{\chi_M} = (H - H_c) \frac{f_G(z)}{f_\chi(z)}. \quad (2.5)$$

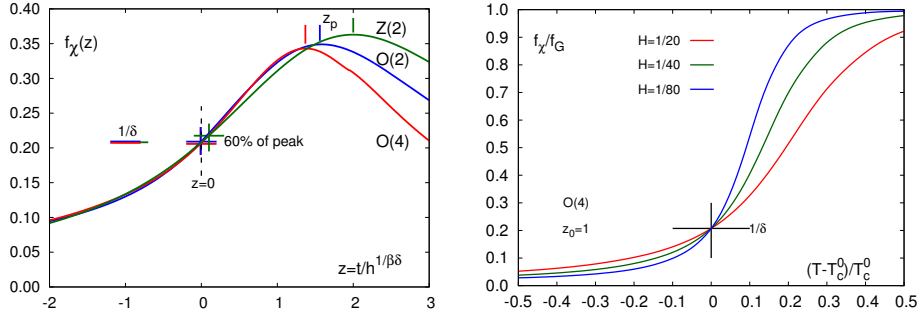


Figure 2: Left: Scaling function f_χ for $O(4)$, $O(2)$ and $Z(2)$ universality classes, z_p is the peak position of f_χ . $z_0 \approx 0$ for these universality classes. Right: Ratio of scaling functions using $O(4)$ exponents for three different values of H [9].

In the case of $m_s^{\text{tri}} < m_s^{\text{phy}}$, H_c is zero and the chiral phase transition is a second order phase transition in the chiral limit, the universality class is expected to be $O(4)$. In the case of $m_s^{\text{phy}} < m_s^{\text{tri}}$, H_c is nonzero and the chiral phase transition is a first order phase transition in the chiral limit, where the corresponding universality class of the second order phase transition occurring at some $H_c > 0$ is $Z(2)$. Since $f_G(z)/f_\chi(z)$ at $z \simeq 0$ and z_p is a number fixed by universality class, one can study the order of the chiral phase transition through the relation between M/χ_M and H at T_{60} and T_{pc} .

3. Lattice setup

In our simulations of (2 + 1)-flavor QCD we have used Highly Improved Staggered Quarks and tree-level improved gauge action (HISQ/tree). The strange quark mass is chosen to its physical quark mass value m_s^{phy} , and the light quark masses values are varied from $m_s^{\text{phy}}/160$ to $m_s^{\text{phy}}/20$ which correspond to $55 \text{ MeV} \leq m_\pi \leq 160 \text{ MeV}$. To perform the continuum limit, the temporal extent N_τ is taken to be 6, 8 and 12 and the spatial volumes used are in the range $4 \leq N_\sigma/N_\tau \leq 8$.

As shown in the Table 2, for each data set we have performed at least 10000 time units (TUs) at each temperature, where gauge configurations are separated by every 5 TUs. We used 50 random noise vectors on each gauge field configuration and constructed unbiased estimators for the various traces to compute the chiral condensate and its susceptibility.

$N_\sigma^3 \times N_\tau$	$\frac{m_l}{m_s^{\text{phy}}}$	average # of TU	$N_\sigma^3 \times N_\tau$	$\frac{m_l}{m_s^{\text{phy}}}$	average # of TU	$N_\sigma^3 \times N_\tau$	$\frac{m_l}{m_s^{\text{phy}}}$	average # of TU
$24^3 \times 6$	1/20	23000	$24^3 \times 8$	1/40	100000	$42^3 \times 12$	1/40	50000
$24^3 \times 6$	1/27	13800	$32^3 \times 8$	1/40	32000	$60^3 \times 12$	1/40	32000
$32^3 \times 6$	1/40	20000	$40^3 \times 8$	1/40	14000	$48^3 \times 12$	1/80	37000
$40^3 \times 6$	1/60	15000	$32^3 \times 8$	1/80	80000	$60^3 \times 12$	1/80	18000
$24^3 \times 6$	1/80	40000	$40^3 \times 8$	1/80	35000	$72^3 \times 12$	1/80	15000
$32^3 \times 6$	1/80	26000	$56^3 \times 8$	1/80	20000			
$48^3 \times 6$	1/80	10000	$56^3 \times 8$	1/160	14000			

Table 2: Current statistics for $N_\tau = 6, 8$ and 12 lattices.

4. Results

We study the subtracted chiral order parameter M and its susceptibility χ_M . To avoid the distortion of the temperature dependence at low temperatures of the chiral order parameter we use

the following definitions

$$M = m_s \left(\langle \bar{\psi}\psi \rangle_l - \frac{2m_l}{m_s} \langle \bar{\psi}\psi \rangle_s \right) / f_K^4, \quad f_K = (156.1/\sqrt{2}) \text{ MeV}, \quad (4.1)$$

$$\chi_M \equiv \frac{\partial M}{\partial H} \equiv m_s^2 \chi_{l,\text{subtot}} / f_K^4, \quad \chi_{l,\text{subtot}} = \frac{\partial}{\partial m_l} \left(\langle \bar{\psi}\psi \rangle_l - \frac{2m_l}{m_s} \langle \bar{\psi}\psi \rangle_s \right). \quad (4.2)$$

We replace the factors of T^4 by the appropriate factors of the kaon decay constant, f_K^4 .

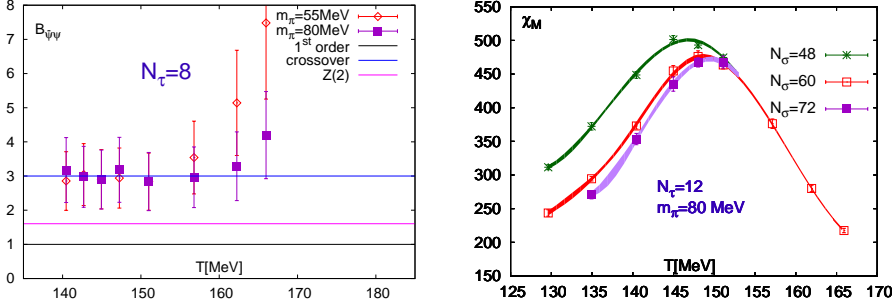


Figure 3: Left: Binder cumulant of chiral condensate on $N_\tau = 8$ lattices for $m_s/m_l = 80$ and 160. Right: Volume dependence of chiral susceptibilities on $N_\tau = 12$ lattices for $m_s/m_l = 80$.

In the left panel of Fig. 3 we show the Binder cumulant of chiral condensate on $N_\tau = 8$ lattices for $m_\pi = 80$ and 55 MeV. Here the Binder cumulant is defined as $B_X = \langle (X - \langle X \rangle)^4 \rangle / \langle (X - \langle X \rangle)^2 \rangle^2$. The plot shows that there is no evidence of first order phase transition in our current pion mass window $55 \text{ MeV} \leq m_\pi \leq 160 \text{ MeV}$. Also as seen from the right panel of Fig. 3, chiral susceptibilities obtained on $N_\tau = 12$ lattices do not grow linearly with the volume which implies that there is no first order phase transition in our current pion mass window. We also observe that T_{pc} is larger for larger volume.

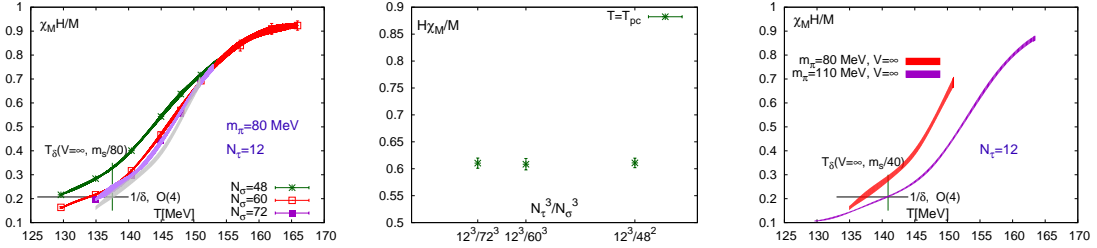


Figure 4: Volume dependence of $\chi_M H/M$ on $N_\tau = 12$ lattices.

We then show the volume dependence of $\chi_M H/M$ in Fig. 4. At a fixed temperature $H\chi_M/M$ becomes smaller in larger volume, and for a fixed volume it increases with increasing temperature. $H\chi_M/M$ at T_{pc} is almost volume independent as shown in the middle plot of Fig. 4. Similar results are also obtained from $N_\tau = 12$ lattices with $m_l = m_s/40$ and $N_\tau = 8$ lattices with $m_l = m_s/80$. As shown in the left plot of Fig. 4, $T_\delta(V, H)$ increases with the increasing volume. Thus, we performed $1/V$ extrapolation as represented by the grey band. This gives $T_\delta(V \rightarrow \infty, m_l = m_s/80) \approx 138 \text{ MeV}$. Similar analyses are done for $m_s/40$ which gives $T_\delta(V \rightarrow \infty, m_l = m_s/40) \approx 141 \text{ MeV}$ as shown as the vertical line in the right plot of Fig. 4. This figure also shows that results for different quark

masses do not cross at a unique point $(T_c, 1/\delta)$ as one would expect in the scaling regime (see Fig. 2(right)). This reflects the importance of regular contributions. We then take the chiral limit by performing linear extrapolation in H , which gives an estimate $T_c^0(N_\tau = 12) \simeq 134(2)$ MeV.

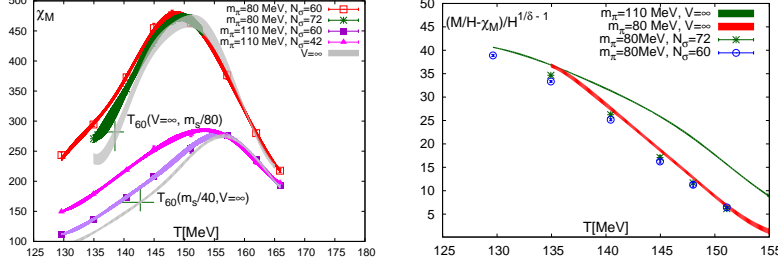


Figure 5: Left: T_{60} for $N_\tau = 12$ lattices. Right: T_c^0 estimated by the crossing point of $M/H - \chi_M$ rescaled by $H^{1/\delta-1}$

In the left plot of Fig. 5 we show the extraction of T_{60} on $N_\tau = 12$ lattices. We performed the $1/V$ extrapolation as shown as the grey bands, and then performed linear chiral extrapolation which gives a consistent result $T_c^0 \approx 134(2)$ MeV. A sanity check for the T_c^0 is to look at the crossing point of $M/H - \chi_M$ rescaled by $H^{1/\delta-1}$. The advantage of $M/H - \chi_M$ is that it removed the regular contributions linear in H . As shown in the right plot of Fig. 5, $(M/H - \chi_M)/H^{1/\delta-1}$ in the infinite volume limit with $H = 1/40$ (the green band) and $H = 1/80$ (the red band) meet at a "crossing point" which is roughly around 135 MeV. Similar procedures e.g. $(T_\delta, T_{60}, M/H - \chi_M)$ are done for $N_\tau = 8$ and 6 which gives $T_c^0 = 142(2)$ and $147(2)$ MeV, respectively. Rather than doing $1/V$ and linear in H extrapolations we also analyze the finite size scaling using $O(4)$ scaling functions, and the continuum extrapolated T_c values are systematically lower by 2-3 MeV which is one source of our systematic uncertainty. The continuum extrapolations discarding results obtained on $N_\tau = 6$ lattices gives about 3 MeV lower T_c^0 , this is another source of our systematic uncertainty.

To study the nature the chiral phase transition, we look at the ratio M/χ_M (c.f. Eq. 2.5). We show the quark mass dependence of M/χ_M at T_{pc} and T_{60} in the left plot and right plot of Fig. 6, respectively. As discussed before, $H\chi_M/M$ at T_{pc} is almost volume independent, and this indicates that all the data points shown in the Fig. 6 can be regarded as being in the infinite volume limit. The colored band in the plots represents the difference between $O(2)$ and $O(4)$ universality classes. In Fig. 6 we also compare our lattice results on the quark mass dependence of M/χ_M with the scenarios of $Z(2)$ phase transition with non-zero H_c corresponding to $m_l/m_s = 1/120$ and $m_l/m_s = 1/240$. As one can see from the figure our lattice results are way above these expectations. Thus, if there is a first order phase transition in the chiral limit of (2 + 1)-flavor QCD, it should happen for quark masses smaller than $m_s/160$.

5. Summary

We have performed lattice simulations of (2 + 1)-flavor QCD using HISQ/tree action. To study the chiral phase transition temperature T_c^0 in the chiral & continuum limit, the light quark mass window was chosen to be $m_s^{\text{phy}}/160 \leq m_l \leq m_s^{\text{phy}}/20$, which correspond to the pion mass window $55 \text{ MeV} \leq m_\pi \leq 160 \text{ MeV}$, N_τ was set to 6, 8, and 12, and the corresponding N_σ ranging from $4N_\tau$ to $8N_\tau$. The current estimates of T_c^0 on $N_\tau = 6, 8$ and 12 lattices are $147(2)$ MeV, $142(2)$

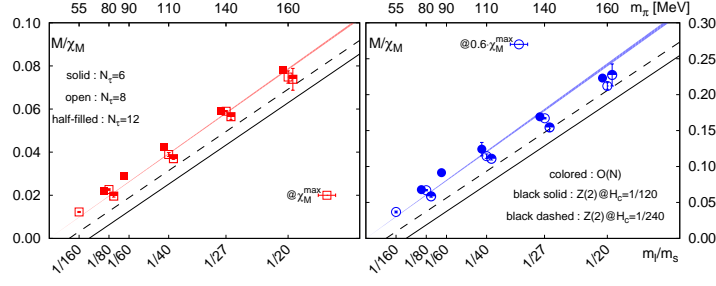


Figure 6: M/χ_M is plotted for different N_τ along with the scaling expectations from different universality classes.

MeV and 135(3) MeV, respectively. Including all systematic uncertainties, our current estimate of T_c^0 in the continuum limit is $T_c^0 = 132_{-6}^{+3}$ MeV [12]. By looking at the ratio M/χ_M as a function of light quark mass, the chiral phase transition is more like a second order phase transition instead of a first order phase transition.

References

- [1] H.-T. Ding, F. Karsch and S. Mukherjee, *Thermodynamics of strong-interaction matter from Lattice QCD*, *Int. J. Mod. Phys. E* **24** (2015) 1530007 [1504.05274].
- [2] R. D. Pisarski and F. Wilczek, *Remarks on the chiral phase transition in chromodynamics*, *Phys. Rev. D* **29** (1984) 338.
- [3] HOTQCD COLLABORATION collaboration, A. Bazavov, T. Bhattacharya, M. Cheng, C. DeTar, H.-T. Ding, S. Gottlieb et al., *Chiral and deconfinement aspects of the qcd transition*, *Phys. Rev. D* **85** (2012) 054503.
- [4] Y. Aoki, G. Endrődi, Z. Fodor, S. D. Katz and K. K. Szabó, *The order of the quantum chromodynamics transition predicted by the standard model of particle physics*, *Nature* **443** (2006) 675 EP.
- [5] A. Bazavov et al., *Chiral crossover in QCD at zero and non-zero chemical potentials*, 1812.08235.
- [6] O. Philipsen and C. Pinke, *$N_f = 2$ qcd chiral phase transition with wilson fermions at zero and imaginary chemical potential*, *Phys. Rev. D* **93** (2016) 114507.
- [7] BIELEFELD-BNL-CCNU collaboration, H.-T. Ding and P. Hegde, *Chiral phase transition of $N_f=2+1$ and 3 QCD at vanishing baryon chemical potential*, *PoS LATTICE2015* (2016) 161 [1511.00553].
- [8] S.-T. Li and H.-T. Ding, *Chiral phase transition of $(2 + 1)$ -flavor QCD on $N_\tau = 6$ lattices*, *PoS LATTICE2016* (2017) 372 [1702.01294].
- [9] H. T. Ding, P. Hegde, F. Karsch, A. Lahiri, S. T. Li, S. Mukherjee et al., *Chiral phase transition of $(2+1)$ -flavor QCD*, *Nucl. Phys. A* **982** (2019) 211 [1807.05727].
- [10] S. Ejiri, F. Karsch, E. Laermann, C. Miao, S. Mukherjee, P. Petreczky et al., *Magnetic equation of state in $(2 + 1)$ -flavor qcd*, *Phys. Rev. D* **80** (2009) 094505.
- [11] F. Karsch and E. Laermann, *Susceptibilities, the specific heat, and a cumulant in two-flavor qcd*, *Phys. Rev. D* **50** (1994) 6954.
- [12] H. T. Ding et al., *The chiral phase transition temperature in $(2+1)$ -flavor QCD*, 1903.04801.